A

FtsH

MNRVFRNTIFYLLILLVVIGVVSYFQTSNPKTENMSYSTFIKNLDDGKVDSVSVQP
VRGVYEVKGQLKNYDKDQYFLTHVPEGKGADQIFNALKKTDVKVEPAQETSGWVTF
LTTIIPFVIIFILFFFLLNQAQGGGSRVMNFGKSKAKLYTEEKKRVKFKDVAGADE
EKQELVEVVEFLKDPRKFAELGARIPKGVLLVGPPGTGKTLLAKACAGEAGVPFFS
ISGSDFVEMFVGVGASRVRDLFENAKKNAPCLIFIDEIDAVGRQRGAGLGGGHDER
EQTLNQLLVEMDGFSANEGIIIIAATNRADILDPALLRPGRFDRQITVDRPDVIGR
EAVLKVHARNKPLDETVNLKSIAMRTPGFSGADLENLLNEAALVAARQNKKKIDAR
DIDEATDRVIAGPAKKSRVISKKERNIVAYHEGGHTVIGLVLDEADMVHKVTIVPR
GQAGGYAVMLPREDRYFQTKPELLDKIVGLLGGRVAEEIIFGEVSTGAHNDFQRAT
NIARRMVTEFGMSEKLGPLQFGQSQGGQVFLGRDFNNEQNYSDQIAYEIDQEIQRI
IKECYERAKQILTENRDKLELIAQTLLKVETLDAEQIKHLIDHGTLPERNFSDDEK
NDDVKVNILTKTEEKKDDTKE

B

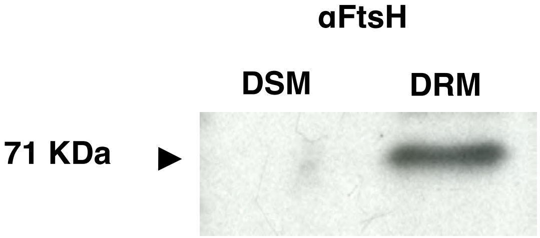

Figure S1: Detection of FtsH in the DRM fraction by mass spectrometry and western blot analysis. (A) Amino acid sequence of FtsH from *B. subtilis*. The oligopeptides from FtsH that were identified in the sample by mass spectrometry analysis are underlined. **(B)** Detection of FtsH by western blot analysis in of the DRM and DSM fraction using polyclonal antibodies against FtsH. The signal was only detected in the DRM fraction. Arrow indicates the molecular weight marker of 71 KDa.

Figure S1

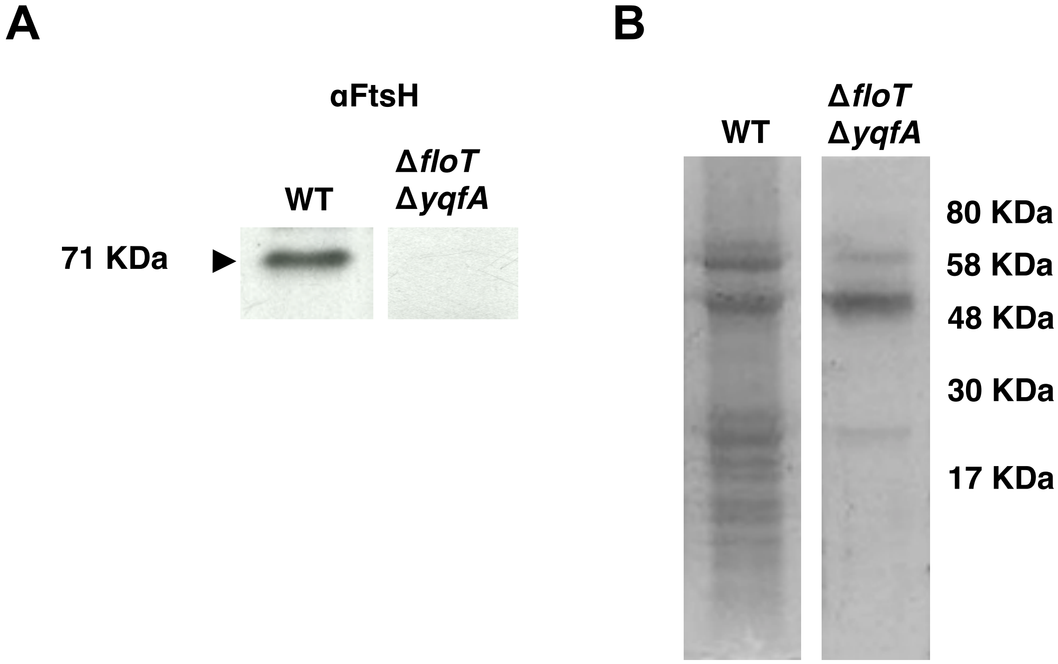

Figure S2: Proteins associated to the DRM fraction decreased in the absence of the flotillin homologs. (A) Western blot analysis using polyclonal antibodies against FtsH to detect the presence of FtsH in the DRM fraction of the wild type strain and the Δ*floT* Δ*yqfA* mutant. Signal was only detected in the DRM fraction of the wild type strain. The arrow indicates the molecular weight expected for FtsH protein. **(B)** SDS-PAGE showing the pool of proteins associated with the membrane fraction that is resistant to detergent solubilization (DRM). The panel shows samples from the wild type strain and in the double Δ*floT* Δ*yqfA* mutant. The protein pattern was analyzed by coomassie staining. Molecular weights are labeled on the right. The protein content of the DRM fractions decreases in the absence of the flotillin-like proteins FloT and YqfA.

Figure S2

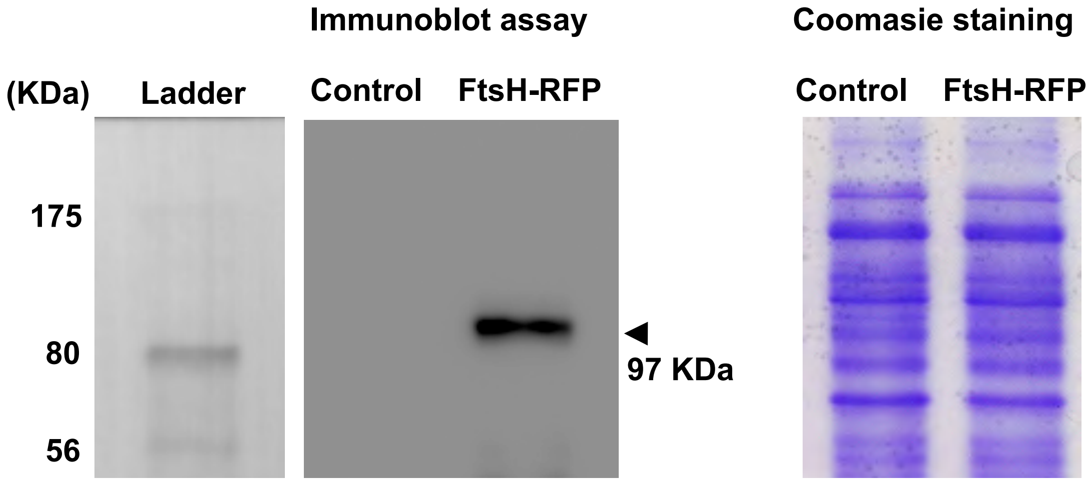

Figure S3: FtsH-RFP is not subject to proteolytic cleavage. Western blot analysis using polyclonal antibodies against RFP to detect the expression and the molecular weight of the translational fusion FtsH-RFP (MW_{FtsH} = 71 KDa + MW_{RFP} = 26 KDa; Total 97 KDa). Negative control in the immunoblot assay is represented by wild-type cell extracts expressing no translational fusion (left lane). The right lane shows the immunoblot analysis extracts from the Δ*ftsH lacA*::P_{hp}-FtsH-RFP strain. The arrow indicates the molecular weight expected for FtsH protein. Coomassie staining of the SDS-PAGE is shown on the right for analysis of the protein content of the cell extracts.

Figure S3

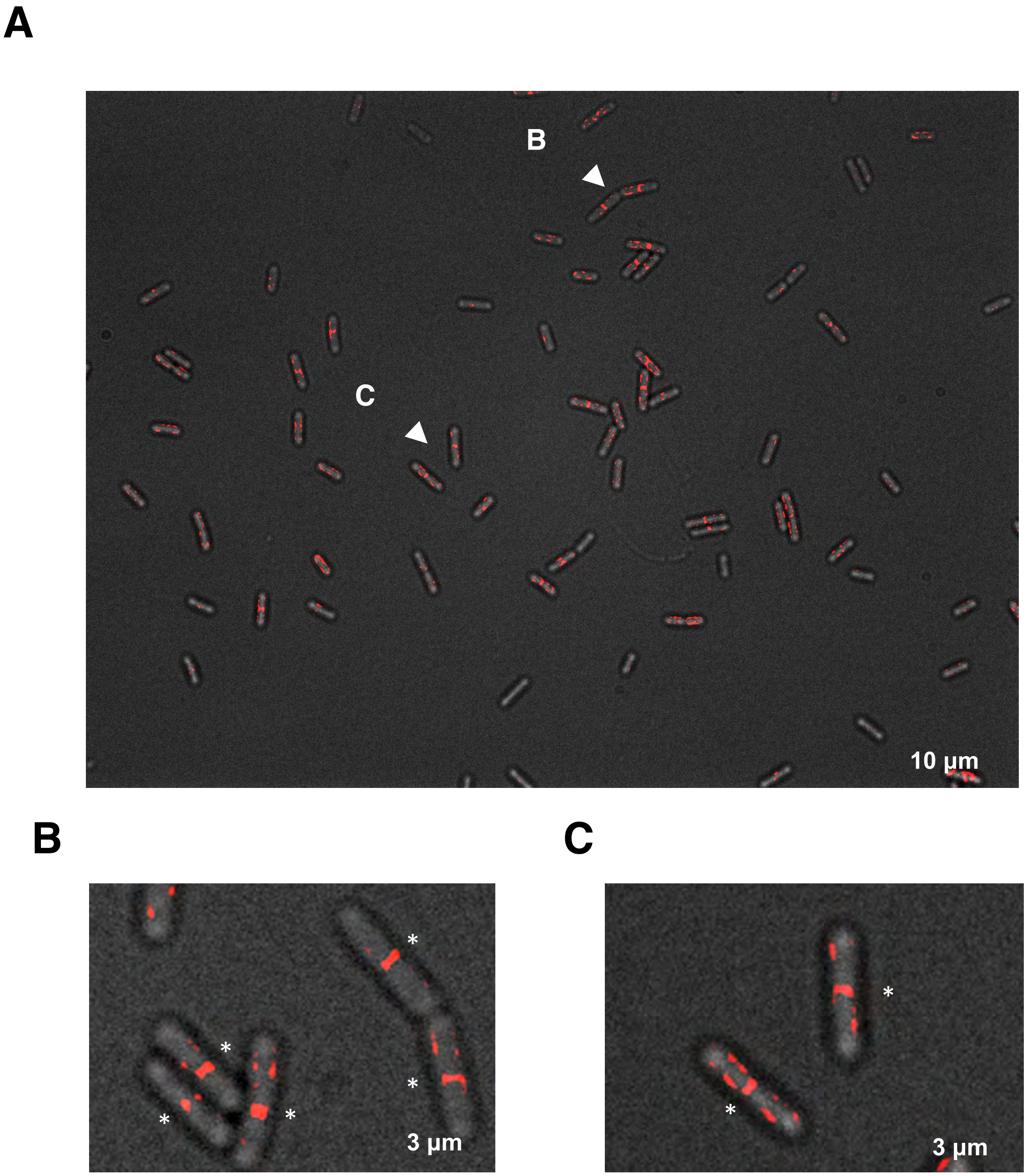

Figure S4: Subcellular localization of the protease FtsH using the translational fusion FtsH-RFP. Fluorescence micrographs of a field of exponentially growing cells labeled with the translational fusion FtsH-RFP (false colored in red). The fluorescence signal shows high concentration in the midcell and lower concentration in certain foci across the cellular membrane. Cells were grown in liquid shaking MSgg at 30°C and cells were harvested in the middle of the exponential phase (approx. 8h of incubation). Arrows indicate detailed fields that are magnified in panels B and C. Asterisks in panels B and C show the midcell position of the signal FtsH-RFP in some cells. The expression of FtsH-RFP was controlled by an IPTG-inducible promoter (induction with 1mM IPTG).

Figure S4

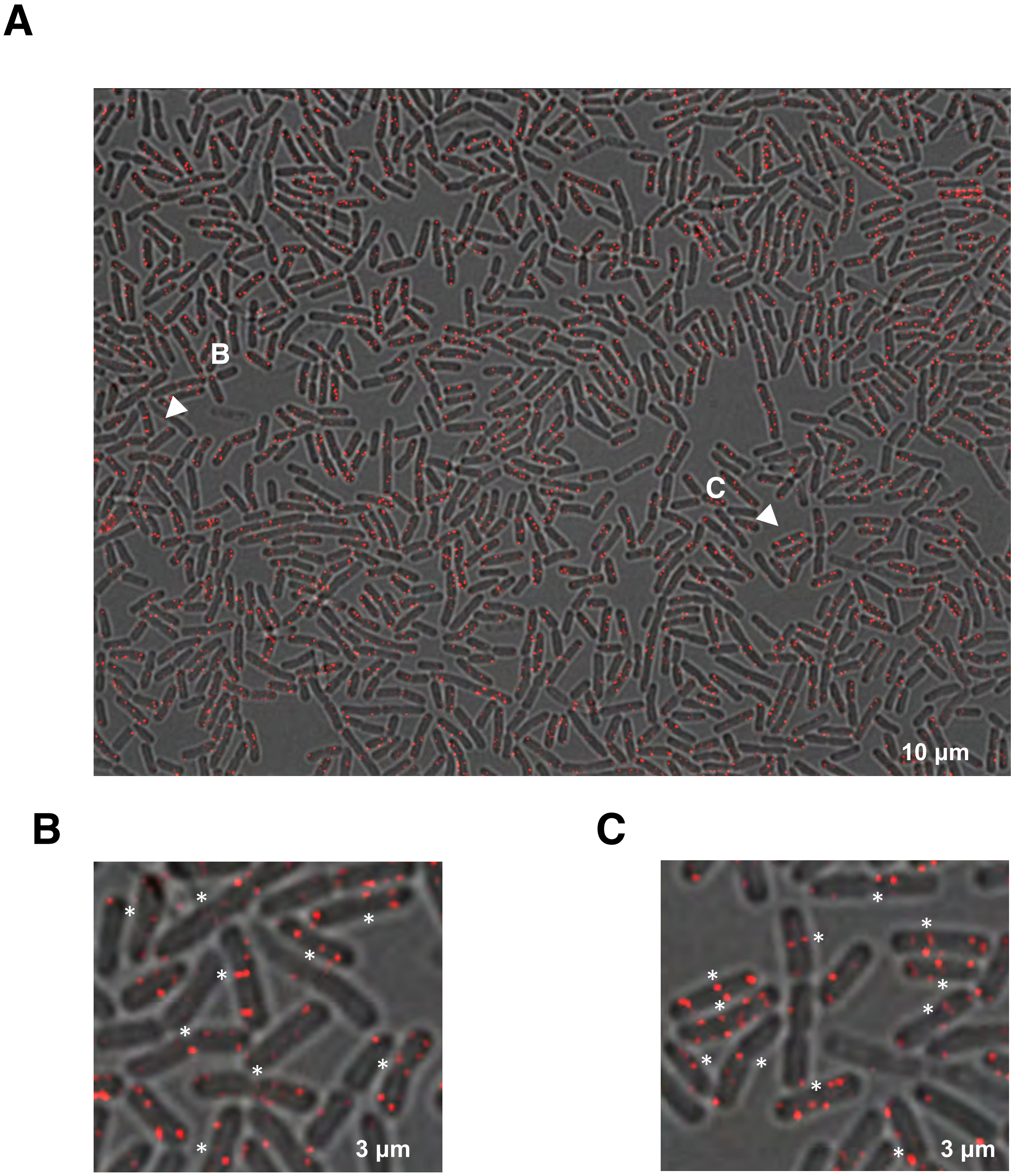

Figure S5: Subcellular localization of the flotillin-like protein FloT using the translational fusion FloT-YFP. Fluorescence micrographs of a field of exponentially growing cells labeled with the translational fusion FloT-YFP (false colored in red). The fluorescence signal shows the typical distribution in foci across the cellular membrane with a high concentration in the midcell. Cells were grown in liquid shaking MSgg at 30°C and cells were harvested in the middle of the exponential phase (approx. 8h of incubation). Arrows indicate detailed fields that are magnified in panels B and C. Asterisks in panels B and C show the midcell position of the signal FloT-YFP in cells.

Figure S5

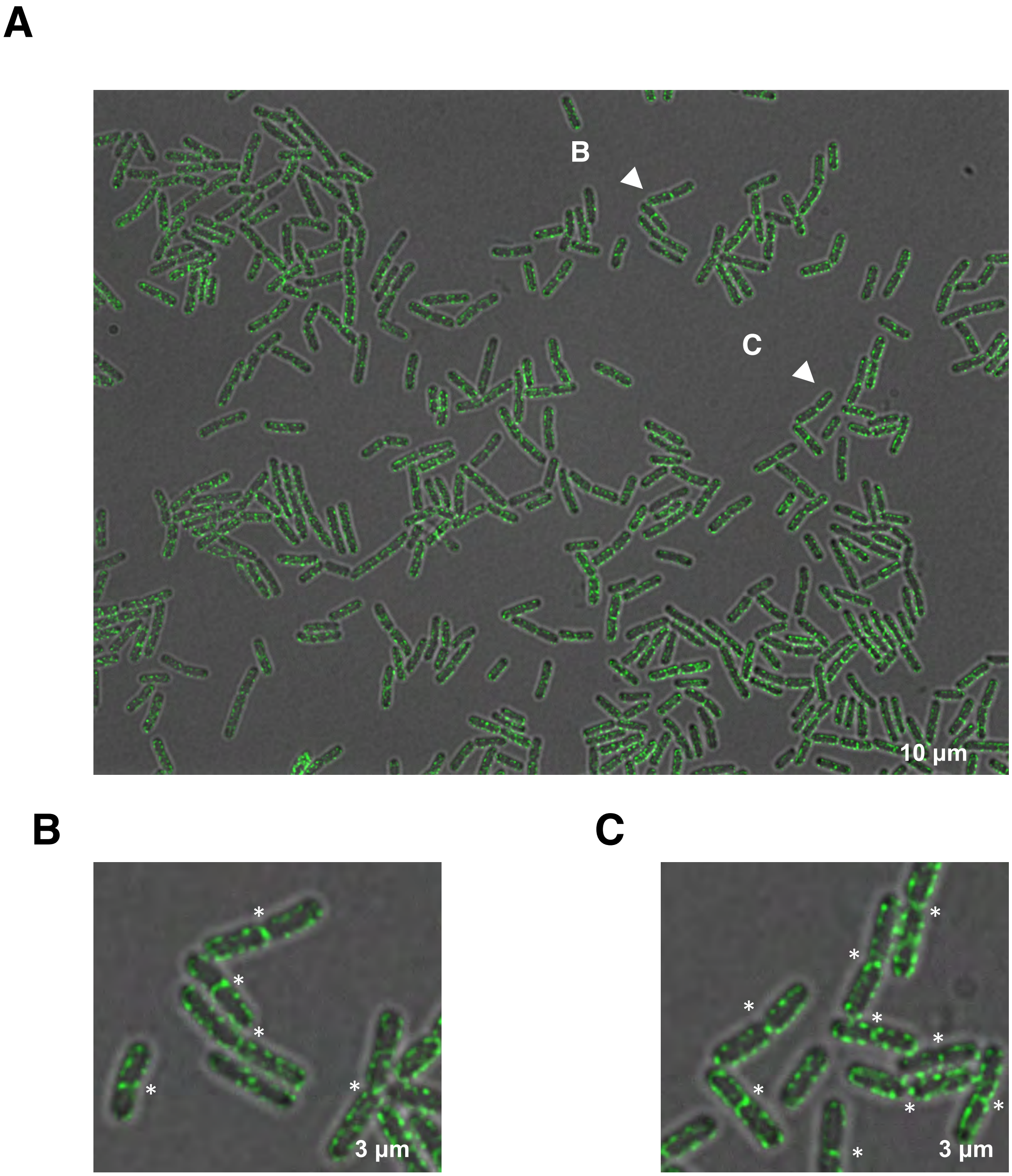

Figure S6: Subcellular localization of the flotillin-like protein YqfA using the translational fusion YqfA-GFP. Fluorescence micrographs of a field of exponentially growing cells labeled with the translational fusion YqfA-GFP (false colored in green). The fluorescence signal shows the typical distribution in foci across the cellular membrane with a high concentration in the midcell. Cells were grown in liquid shaking MSgg at 30°C and cells were harvested in the middle of the exponential phase (approx. 8h of incubation). Arrows indicate detailed fields that are magnified in panels B and C. Asterisks in panels B and C show the midcell position of the signal YqfA-GFP in cells.

Figure S6

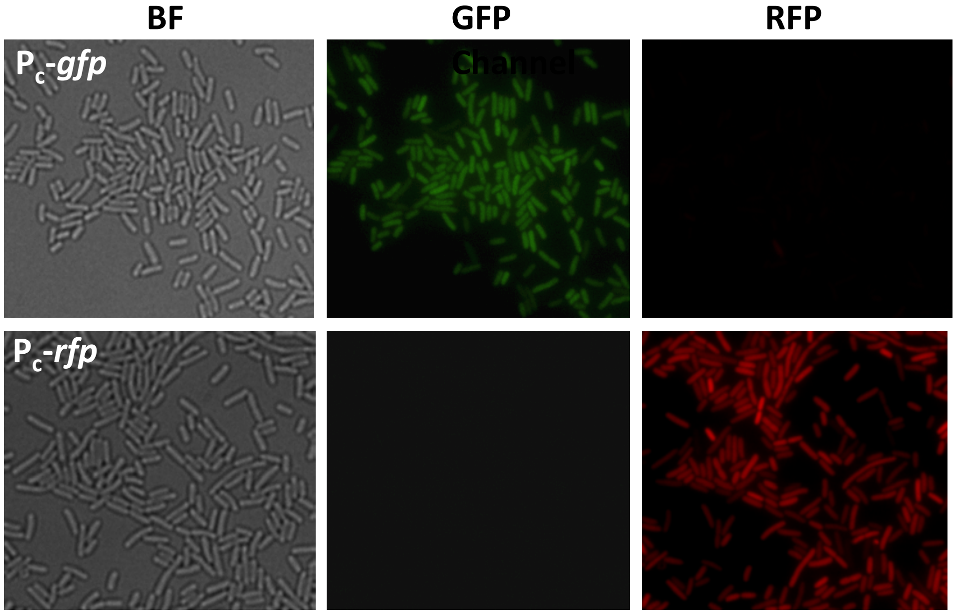

Figure S7: There is no interference between the green and red fluorescence signal. Fluorescence micrographs and transmitted light images of *E. coli* strains grown in liquid shaking LB at 37°C for 24h. The strains expressed GFP (upper row) or RFP (bottom row) under the control of a constitutive promoter (P_c). scale bar is 5 µm. Fluorescence signal detected in the green and red channel are presented in GFP and RFP labeled columns, respectively. Transmitted light images are presented in the column labeled as BF.

Figure S7

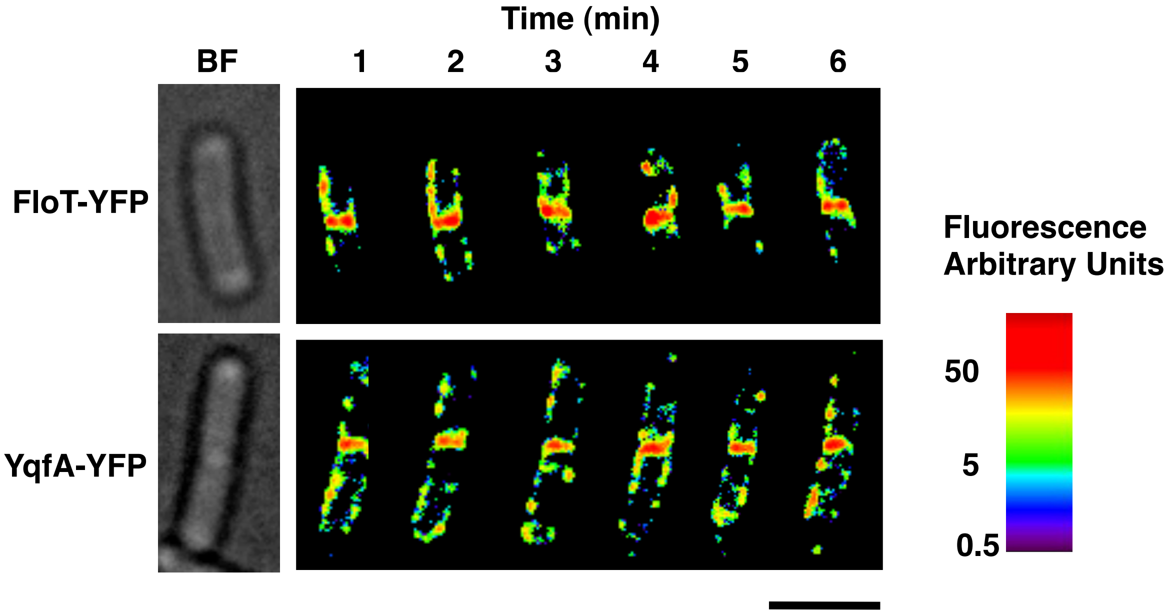

Figure S8: Flotillins are permanently present at the midcell. Time-lapse fluorescence analysis of the distribution pattern of FloT-YFP and YqfA-GFP foci. Cells were grown in liquid shaking MSgg at 30°C for 8h. Exponentially growing cells were mounted on agarose-coated slides. The upper row shows the distribution of the FloT–YFP foci within the same cell for 6 min. The bottom row shows the distribution of the YqfA–GFP foci within the same cell for 6 min. This figure corresponds to figure 7 of the body of the paper. Fluorescence signal is quantified in relation to the background fluorescence using a color spectrum logarithmic scale, in which higher intensity of the fluorescence signal is represented in red tones (scale is presented on the right). Scale bar is 2 μm.

Figure S8

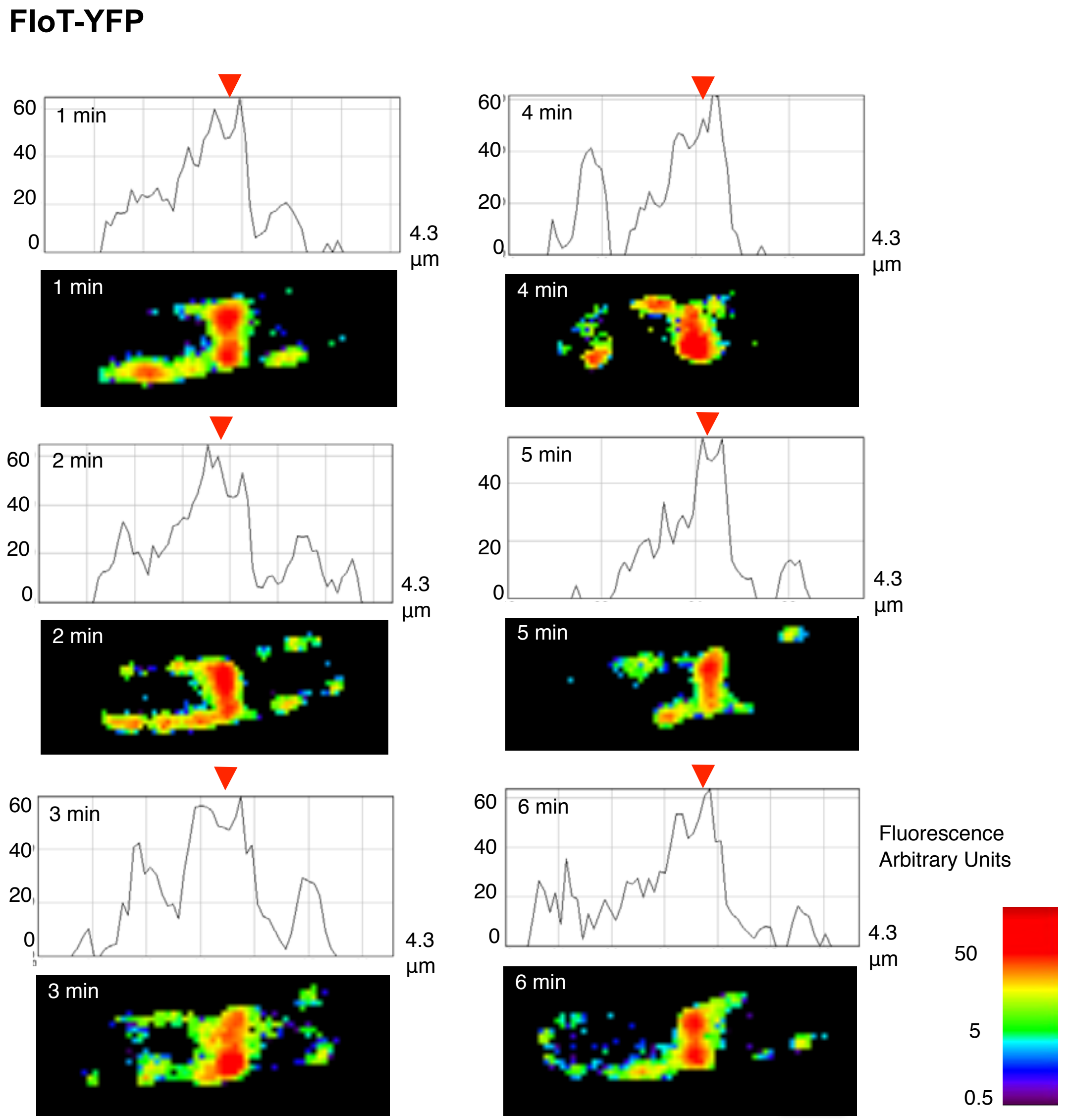

Figure S9: Quantification of relative fluorescence intensity detected in the time-lapse fluorescence analysis of FloT-YFP. Time-lapse fluorescence analysis of the distribution pattern of FloT-YFP foci for a time period of 6 min. Each panel shows a detailed micrograph of the distribution of the FloT–YFP foci within the same cell at every point (in min). Fluorescence signal is quantified in relation to the background fluorescence, using a color spectrum logarithmic scale (spectrum scale is presented on the right). The relative fluorescence intensity values of each micrograph is represented in a graph (above each micrograph). X-axis represents the cell length and y-axis represents the value of relative fluorescence intensity detected. The midcell is marked with a red arrow. Scale bar is 1 µm.

Figure S9

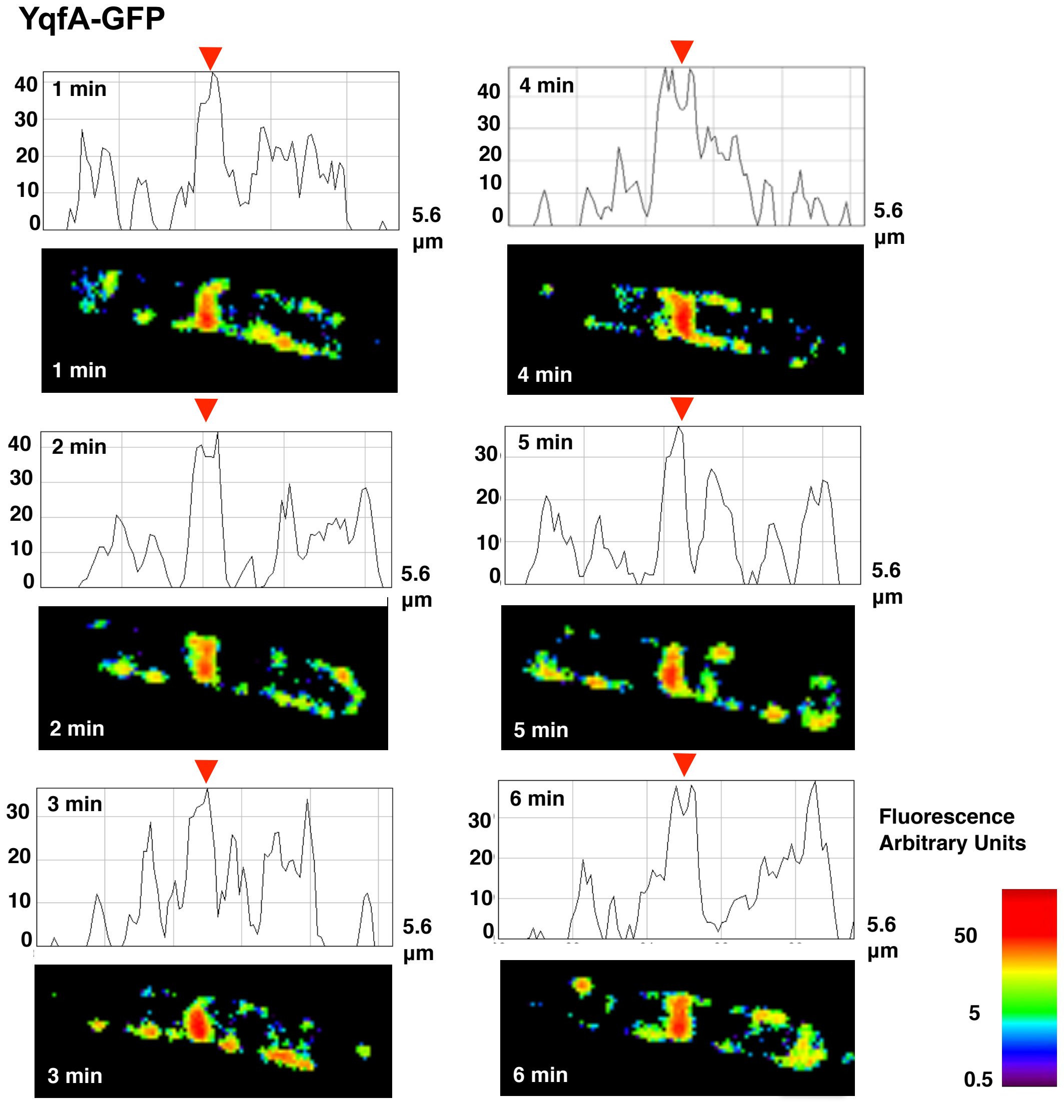

Figure S10: Quantification of relative fluorescence intensity detected in the time-lapse fluorescence analysis of YqfA-GFP. Time-lapse fluorescence analysis of the distribution pattern of YqfA-GFP foci for a time period of 6 min. Each panel shows a detailed micrograph of the distribution of the YqfA–GFP foci within the same cell at every point (in min). Fluorescence signal is quantified in relation to the background fluorescence, using a color spectrum logarithmic scale (spectrum scale is presented on the right). The relative fluorescence intensity values of each micrograph is represented in a graph (above each micrograph). X-axis represents the cell length and y-axis represents the value of relative fluorescence intensity detected. The midcell is marked with a red arrow. Scale bar is 1 µm.

Figure S10

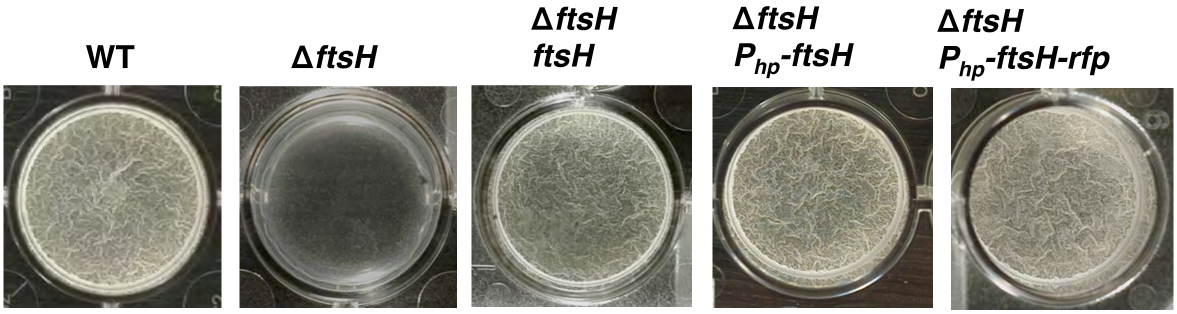

Figure S11: Complementation of the Δ*ftsH* mutant with a wild-type copy of *ftsH* restored biofilm formation. Pellicle formation assay of different strains of *B. subtilis*. Pictures show a top view of the pellicles formed on the surface of MSgg liquid cultures incubated in 24-well plates at 30°C for 24h. Positive control is represented by the wild-type strain (WT) (left panel). Δ*ftsH* mutant shows no pellicle formation (second panel). Complementation of Δ*ftsH* mutant with a copy of *ftsH* induced by its own promoter partially restored biofilm formation (third panel). Complementation of Δ*ftsH* mutant with an IPTG-inducible copy of *ftsH* restored wild-type levels of biofilm formation. Similar results were obtained when the Δ*ftsH* mutant was complemented with the translational fusion FtsH-RFP (right panel). IPTG was added to a final concentration of 1mM.

Figure S11

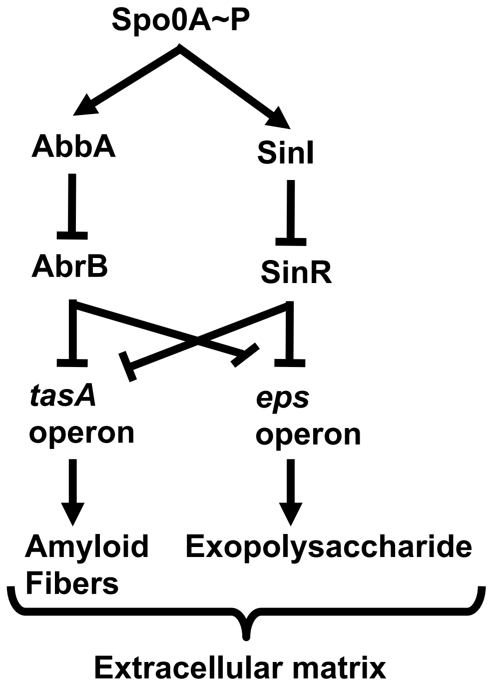

Figure S12: Flow scheme of the regulatory circuit involved in extracellular matrix production. Arrows indicate activation of transcription and T bars indicate repression. AbrB and SinR are two regulatory repressors that independently repress the genes required for the production of amyloid fibers and exopolysaccharide production. Both exopolysacchride and amyloid fibers are important constituent of the extracellular matrix of the biofilm. Repression of AbrB and SinR expression is driven by the activation of the master regulator Spo0A~P.

Figure S12

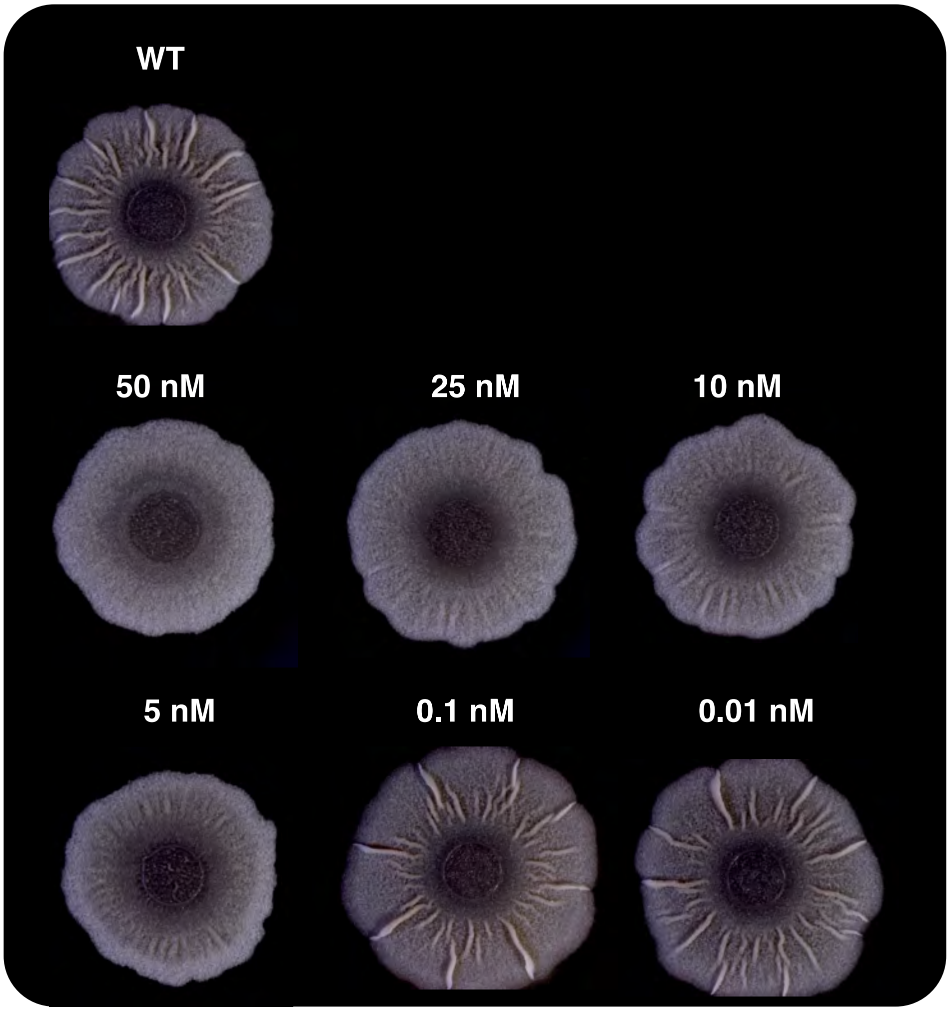

Figure S13: Colony morphology assay of *B. subtilis* NCIB3610 in the presence of a range of concentrations of the SpoVM protein. The ability of *B. subtilis* 3610 to make biofilm in solid MSgg agar can be correlated to the amount of wrinkles that are present in the surface of the colony. Addition of small concentrations of SpoVM inhibited the formation of wrinkles, which is indicative of an inhibition of biofilm formation. Gradual decrease of the concentration of SpoVM restored the formation of wrinkles in the colonies of *B. subtilis*. Colonies were incubated in MSgg agar at at 30°C for 72h.

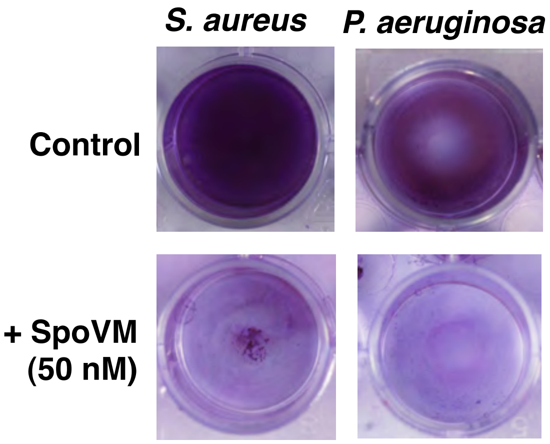

Figure S14: SpoVM inhibits biofilm formation. Biofilm formation assay of *S. aureus* SC-01 and *P. aeruginosa* PA14. 1ml of the culture was dispensed in polystyrene well plates and incubated overnight at 37° C. Biofilms were stained with crystal violet for better visualization. Addition of 50 nM of the peptide SpoVM inhibited the ability of both strains to form biofilm attached to the bottom of the well, evidenced by the absence of crystal violet dye after staining.

Table S1: Proteins associated with the DRM fraction in *B. subtilis*

Protein	**Function**	**Functional Category**
FtsH	Metalloprotease	Cell shape
MreBH	Actin-like protein	
MreC	Actin-associated protein	
EzrA	Tubulin-associated protein	
OppA	Oligopeptide ABC transporter	Quorum sensing
PrsA	Protease secretion chaperone.	Protease secretion
FeuA	Iron-uptake system (binding protein)	Iron uptake
FeuB	Iron-uptake system (membrane protein)	
PbpC	Penicillin-binding protein 3	Penicillin-binding proteins
DacA	Penicillin-binding protein 5	
DacC	Penicillin-binding protein	
YxeB	Unknown. Similar to ABC transporter	Unknown
YwjA	Unknown. Similar to ABC transporter	
YknZ	Unknown. Similar to ABC transporter	
YwbM	Unknown	
YcdA	Unknown	
YerH	Unknown	
YufN	Unknown	
AdcA	Lipoprotein	Transporter
BdbD	Thiol-disulfide oxidorreductase	Protein folding
Qox2	Quinol oxidase	Redox enzyme
YxeM	ABC transporter	Transporter
RbsB	ABC transporter	Transporter
YkwC	Unknown	Unknown
YeeF	Unknown	
YpuA	Unknown	

Table S1 (continuation): Proteins associated with the DRM fraction in *B. subtilis*

Amino acid sequence of the proteins listed in table S1. The oligopeptides that were identified in the samples by mass spectrometry analysis are underlined. The percentage coverage value obtained for each protein is shown in parenthesis.

FtsH (38.93 %)
MNRVFRNTIFYLLILLVVIGVVSYFQTSNPKTENMSYSTFIKNLDDGKVDSVSVQPVRGVYEVKGQLKNYD
KDQYFLTHVPEGKGADQIFNALKKTDVKVEPAQETSGWVTFLTTIIPFVIIFILFFFLLNQAQGGGSRVMN
FGKSKAKLYTEEKKRVKFKDVAGADEEKQELVEVVEFLKDPRKFAELGARIPKGVLLVGPPGTGKTLLAKA
CAGEAGVPFFSISGSDFVEMFVGVGASRVRDLFENAKKNAPCLIFIDEIDAVGRQRGAGLGGGHDEREQTL
NQLLVEMDGFSANEGIIIIAATNRADILDPALLRPGRFDRQITVDRPDVIGREAVLKVHARNKPLDETVNL
KSIAMRTPGFSGADLENLLNEAALVAARQNKKKIDARDIDEATDRVIAGPAKKSRVISKKERNIVAYHEGG
HTVIGLVLDEADMVHKVTIVPRGQAGGYAVMLPREDRYFQTKPELLDKIVGLLGGRVAEEIIFGEVSTGAH
NDFQRATNIARRMVTEFGMSEKLGPLQFGQSQGGQVFLGRDFNNEQNYSDQIAYEIDQEIQRIIKECYERA
KQILTENRDKLELIAQTLLKVETLDAEQIKHLIDHGTLPERNFSDDEKNDDVKVNILTKTEEKKDDTKE

MreBH (48.06 %)
MFQSTEIGIDLGTANILVYSKNKGIILNEPSVVAVDTTTKAVLAIGADAKNMIGKTPGKIVAVRPMKDGVI
ADYDMTTDLLKHIMKKAAKSIGMSFRKPNVVVCTPSGSTAVERRAISDAVKNCGAKNVHLIEEPVAAAIGA
DLPVDEPVANVVVDIGGGTTEVAIISFGGVVSCHSIRIGGDQLDEDIVSFVRKKYNLLIGERTAEQVKMEI
GHALIEHIPEAMEIRGRDLVTGLPKTIMLQSNEIQDAMRESLLHILEAIRATLEDCPPELSGDIVDRGVIL
TGGGALLNGIKEWLTEEIVVPVHVAQNPLESVAIGTGRSLEVIDKLQKAIK

MreC (52.41 %)
MPNKRLMLLLLCIIILVAMIGFSLKGGRNTTWPEKVIGDTTGVFQNIFHTPAEFFAGIFENINDLKNTYKE
NERLREKLDGQTQYEAKLQELEEENKSLRDELGHVKSIKDYKPILATVIARSPDNWAKQVTINKGTQQNVA
FDMAVTNEKGALIGKIKSSGLNNFTSAVQLLSDPDRNNRVATKISGKKGSKGYGLIEGYDKEKKRLKMTII
ERKDKQDVKKGDLIETSGTGGVFPEGLTIGEVTDIESDSYGLTKVAYVKPAADLTDLNNVIVVNRDVPTVD
TEEEGS

EzrA (52.85 %)
MEFVIGLLIVLLALFAAGYFFRKKIYAEIDRLESWKIEILNRSIVEEMSKIKHLKMTGQTEEFFEKWREEW
DEIVTAHMPKVEELLYDAEENADKYRFKKANQVLVHIDDLLTAAESSIEKILREISDLVTSEEKSREEIEQ
VRERYSKSRKNLLAYSHLYGELYDSLEKDLDEIWSGIKQFEEETEGGNYITARKVLLEQDRNLERLQSYID
DVPKLLADCKQTVPGQIAKLKDGYGEMKEKGYKLEHIQLDKELENLSNQLKRAEHVLMTELDIDEASAILQ
LIDENIQSVYQQLEGEVEAGQSVLSKMPELIIAYDKLKEEKEHTKAETELVKESYRLTAGELGKQQAFEKR
LDEIGKLLSSVKDKLDAEHVAYSLLVEEVASIEKQIEEVKKEHAEYRENLQALRKEELQARETLSNLKKTI
SETARLLKTSNIPGIPSHIQEMLENAHHHIQETVNQLNELPLNMEEAGAHLKQAEDIVNRASRESEELVEQ
VILIEKIIQFGNRFRSQNHILSEQLKEAERRFYAFDYDDSYEIAAAAVEKAAPGAVEKIKADISA

OppA (59.63 %)
MKKRWSIVTLMLIFTLVLSACGFGGSGSNGEGKKDSKGKTTLNINIKTEPFSLHPGLANDSVSGGVIRQTF
EGLTRINADGEPEEGMASKIETSKDGKTYTFTIRDGVKWSNGDPVTAQDFEYAWKWALDPNNESQYAYQLY
YIKGAEAANTGKGSLDDVAVKAVNDKTLKVELNNPTPYFTELTAFYTYMPINKKIAEKNKKWNTNAGDDYV
SNGPFKMTAWKHSGSITLEKNDQYWDKDKVKLKKIDMVMINNNNTELKKFQAGELDWAGMPLGQLPTESLP
TLKKDGSLHVEPIAGVYWYKFNTEAKPLDNVNIRKALTYSLDRQSIVKNVTQGEQIPAMAAVPPTMKGFED
NKEGYFKDNDVKTAKEYLEKGLKEMGLSKASDLPKIKLSYNTDDAHAKIAQAVQEMWKKNLGVDVELDNSE
WNVYIDKLHSQDYQIGRMGWLGDFNDPINFLELFRDKNGGNNDTGWENPEFKKLLNQSQTETDKTKRAELL
KKAEGIFIDEMPVAPIYFYTDTWVQDENLKGVIMPGTGEVYFRNAYFK

PrsA (72.60 %)
MKKIAIAAITATSILALSACSSGDKEVIAKTDAGDVTKGELYTNMKKTAGASVLTQLVQEKVLDKKYKVSD
KEIDNKLKEYKTQLGDQYTALEKQYGKDYLKEQVKYELLTQKAAKDNIKVTDADIKEYWEGLKGKIRASHI
LVADKKTAEEVEKKLKKGEKFEDLAKEYSTDSSASKGGDLGWFAKEGQMDETFSKAAFKLKTGEVSDPVKT
QYGYHIIKKTEERGKYDDMKKELKSEVLEQKLNDNAAVQEAVQKVMKKADIEVKDKDLKDTFNTSSTSNST
SSSSSNSK

FeuA (61.51 %)
MKKISLTLLILLLALTAAACGSKNESTASKASGTASEKKKIEYLDKTYEVTVPTDKIAITGSVESMEDAKL
LDVHPQGAISFSGKFPDMFKDITDKAEPTGEKMEPNIEKILEMKPDVILASTKFPEKTLQKISTAGTTIPV
SHISSNWKENMMLLAQLTGKEKKAKKIIADYEQDLKEIKTKINDKAKDSKALVIRIRQGNIYIYPEQVYFN
STLYGDLGLKAPNEVKAAKAQELSSLEKLSEMNPDHIFVQFSDDENADKPDALKDLEKNPIWKSLKAVKED
HVYVNSVDPLAQGGTAWSKVRFLKAAAEKLTQN

FeuB (38.32 %)
MYSKQWTRIILITSPFAIALSLLLSILYGAKHLSTDIVFTSLIHFDPGNTDHQIIWHSRIPRAAGALLIGA
ALAVSGALMQGITRNYLASPSIMGVSDGSAFIITLCMVLLPQSSSIEMMIYSFIGSALGAVLVFGLAAMMP
NGFTPVQLAIIGTVTSMLLSSLSAAMSIYFQISQDLSFWYSARLHQMSPDFLKLAAPFFLIGIIMAISLSK
KVTAVSLGDDISKSLGQKKKTIKIMAMLSVIILTGSAVALAGKIAFVGLVVPHITRFLVGSDYSRLIPCSC
ILGGIFLTLCDLASRFINYPFETPIEVVTSIIGVPFFLYLIKRKGGEQNG

PbpC (56.14 %)
MLKKCILLVFLCVGLIGLIGCSKTDSPEDRMEAFVKQWNDQQFDDMYQSLTKDVKKEISKKDFVNRYKAIY
EQAGVKNLKVTAGEVDKDDQDNKTMKHIPYKVSMNTNAGKVSFKNTAVLKLEKTDDEESWNIDWDPSFIFK
QLADDKTVQIMSIEPKRGQIYDKNGKGLAVNTDVPEIGIVPGELGDKKEKVIKELAKKLDLTEDDIKKKLD
QGWVKDDSFVPLKKVKPDQEKLVSEATSLQGVTRTNVSSRYYPYGEKTAHLTGYVRAITAEELKKKKEGTY
SDTSNIGIAGLENVYEDKLRGTTGWKIYVPQTGEVIAEKKAKDGEDLHLTIDIKTQMKLYDELKDDSGAAV
ALQPKTGETLALVSAPSYDPNGFIFGWSDKEWKKLNKDKNNPFSAKFNKTYAPGSTIKPIAAAIGIKNGTL
KADEKKTIKGKEWQKDSSWGGYSVTRVSERLQQVDLENALITSDNIYFAQNALDMGADTFTKGLKTFGFSE
DVPYEFPIQKSSIANDKLDSDILLADTGYGQGQMQMSPLHLATAYTPFVDNGDLVKPTLIKKDSQTADVWH
KQVVTKEGAADITKGLKGVVEDERGSAYQPVVKGITVAGKTGTAELKTSKDDKDGTENGWFVGYDYENKDL
LVAMMIQNVQDRGGSHYVVEKAKKQFQSN

DacA (63.66 %)
MNIKKCKQLLMSLVVLTLAVTCLAPMSKAKAASDPIDINASAAIMIEASSGKILYSKNADKRLPIASMTKM
MTEYLLLEAIDQGKVKWDQTYTPDDYVYEISQDNSLSNVPLRKDGKYTVKELYQATAIYSANAAAIAIAEI
VAGSETKFVEKMNAKAKELGLTDYKFVNATGLENKDLHGHQPEGTSVNEESEVSAKDMAVLADHLITDYPE
ILETSSIAKTKFREGTDDEMDMPNWNFMLKGLVSEYKKATVDGLKTGSTDSAGSCFTGTAERNGMRVITVV
LNAKGNLHTGRFDETKKMFDYAFDNFSMKEIYAEGDQVKGHKTISVDKGKEKEVGIVTNKAFSLPVKNGEE
KNYKAKVTLNKDNLTAPVKKGTKVGKLTAEYTGDEKDYGFLNSDLAGVDLVTKENVEKANWFVLTMRSIGG
FFAGIWGSIVDTVTGWF

DacC (26.27 %)
MKKSIKLYVAVLLLFVVASVPYMHQAALAAEKQDALSGQIDKILADHPALEGAMAGITVRSAETGAVLYEH
SGDTRMRPASSLKLLTAAAALSVLGENYSFTTEVRTDGTLKGKKLNGNLYLKGKGDPTLLPSDFDKMAEIL
KHSGVKVIKGNLIGDDTWHDDMRLSPDMPWSDEYTYYGAPISALTASPNEDYDAGTVIVEVTPNQKEGEEP
AVSVSPKTDYITIKNDAKTTAAGSEKDLTIEREHGTNTITIEGSVPVDANKTKEWISVWEPAGYALDLFKQ
SLKKQGITVKGDIKTGEAPSSSDVLLSHRSMPLSKLFVPFMKLSNNGHAEVLVKEMGKVKKGEGSWEKGLE
VLNSTLPEFGVDSKSLVLRDGSGISHIDAVSSDQLSQLLYDIQDQSWFSAYLNSLPVAGNPDRMVGGTLRN
RMKGTPAQGKVRAKTGSLSTVSSLSGYAETKSGKKLVFSILLNGLIDEEDGKDIEDQIAVILANQ

YxeB (60.19 %)
MKKNILLVGMLVLLLMFVSACSGTASKGSSSDSASEKTEMRTYKSPKGNVNIPAHPKRIVTDFYAGELLSV
GANVVGSGSWSFDNPFLKSKLKNVKDVGDPISVEKVMELQPDLIVVMNEENVDKLKKIAPTVVIPYNTAKN
VEDTVSMFGDIAGAKDQAKSFMADFNKKAEAAKKKIAGVIDKDATFGIYENTDKGEFWVFNDNGGRGGQAV
YNALGLKAPEKIEQDVIKKGEMKQLSQEVIPEYAADYMFITDYNPKGESKTLDKLENSSIWKNLDAVKHNR
VFINDFDSFYPYDPISVSKQVDIITDMLIKRAEEN

YwjA (36.17 %)
MLRQFFSYYKPYKTLFFLDFFSAIAGGLMELSFPLIVNYFIDTLLPGRDWGLIIATSIGLFAVYALSSALQ
YIVTYWGHMLGINIETDMRKSLFDHLQKLSFKFYDNNKTGTLMSKLTNDLMYIGEVAHHGPEDLFIAVMTI
LGAFGVMLFINWQLALLTFIIMPIVIWLALYFNKKMTKAFTTLNKDIGDFSARVENNIGGIRLVQAFGNEA
FEKERFAVNNQRFRVTKLSSYKIMAKNGSISYMLTRFVTLFVLLCGTWFVIRGSLSYGEFVAFVLLTNVLF
RPIDKINAIIEMYPRGIAGFKSYMELMETEPDIQDSPDSKDVSGLKGNIRYKHVSFGYDDHHNVLNDINLS
IQAGETVAFVGPSGAGKSTLCSLLPRFYEASEGDITIDGISIKDMTLSSLRGQIGVVQQDVFLFSGTLREN
IAYGRLGASEEDIWQAVKQAHLEELVHNMPDGLDTMIGERGVKLSGGQKQRLSIARMFLKNPSILILDEAT
SALDTETEAAIQKALQELSEGRTTLVIAHRLATIKDADRIVVVTNNGIEEQGRHQDLIEAGGLYSRLHQAQ
FGQMVHR

YknZ (8.8 %)
MSLLENIRMALSSVLAHKMRSILTMLGIIIGVGSVIVVVAVGQGGEQMLKQSISGPGNTVELYYMPSDEEL
ASNPNAAAESTFTENDIKGLKGIEGIKQVVASTSESMKARYHEEETDATVNGINDGYMNVNSLKIESGRTF
TDNDFLAGNRVGIISQKMAKELFDKTSPLGEVVWINGQPVEIIGVLKKVTGLLSFDLSEMYVPFNMMKSSF
GTSDFSNVSLQVESADDIKSAGKEAAQLVNDNHGTEDSYQVMNMEEIAAGIGKVTAIMTTIIGSIAGISLL
VGGIGVMNIMLVSVTERTREIGIRKSLGATRGQILTQFLIESVVLTLIGGLVGIGIGYGGAALVSAIAGWP
SLISWQVVCGGVLFSMLIGVIFGMLPANKAAKLDPIEALRYE

YwbM (78.7 %)
MNFTKIAVSAGCILALCAGCGANDTSSTKEKASSEKSGVTKEITASVNKMETIISKLNDSVEKGDQKEIEK
KGKELNSYWLSFENDIRSDYPFEYTEIEKHLQPIYTEAQKDKPDAGKIKTESESLKASLEDLTEAKKSGKK
ASDQLAKAADEYKGYVKEQSDQLVKATEAFTGAVKSGDIEKSKTLYAKARVYYERIEPIAESLGDLDPKID
ARENDVEEGDKWTGFHKLEKAIWKDQDISGEKATADQLLKDVKELDGSIQSLKLTPEQIVAGAMELLNEAG
ISKITGEEERYSRIDLVDLMANVEGSEAVYQTVKSALVKDHSDLTEKLDTEFSEFEVLMAKYKTNDQSYTS
YDKLSEKQIRELSTKLTTLSETMSKIANVL

YcdA (75.99 %)
MFQKKTYAVFLILLLMMFTAACSGSKTSAEKKESETEKSSDIAQVKIKDVSYTLPSKYDKSTSDDQLVLKV
NVAVKNTGKDPLNVDSMDFTLYQGDTKMSDTDPEDYSEKLQGSTINADKSVEGNLFFVVDKGKQYELNYTP
ESYGDKKPKSVTFKIDGKDKKILATADKLQDSAKALSAYVDVLLFGKDNADFEKITGANKNEIVNDFNESA
KDGYLSASGLSSTYADSKALDNIVNGIKEGLSKNSSIQAKTTSISKDEAIVEATVKPVDASSLSDRIEDKV
KDYYSKNSSASYEEAVKYALQVYPEEFKKLGPASSEKTVEVKMKKNDIDQWQLDMDDYRAAELVEAFIKE

YerH (55.05 %)
MKKTLALAATAAVLMLSACSSGFGGEKEEEITQKTAKSSEKAIVPKYNISDSYYKMVLPFKAGKARGLTTE
QLNTRLDIDEFETGLMRLAQDSFSTDDYLFQEGQYLDEDTVLSWLARKKTGSDLKKAEKEDKNFKNEGLNP
ALPSSGSTEEKNESSPIYLASMLEHDYLVRKDKNSIQLGGVMIGLALNSVYYYREKTGDPQKEVEIKDSTL
RQQGEKIAQEVINRLRKKDNLKNVPITVALYKQASKTSIVPGNFIAKTEVKAGSTDISNWDDINEKYVFYP
ADTTTAEKYPDDTEVFKRFKNSIEEYFPNYTGVVGTALYENDEMKKMKIDIPMQFYGKSEVVAFTQFLTGE
VMDYYSKSSVDVEVNITSSDGQEAVIIRNAGDKEPTVHIYD

YufN (77.14 %)
MSLVIAAGTILGACGNSEKSSGSGEGKNKFSVAMVTDVGGVDDKSFNQSAWEGIQAFGKENGLKKGKNGYD
YLQSKSDADYTTNLNKLARENFDLIYGVGYLMEDSISEIADQRKNTNFAIIDAVVDKDNVASITFKEQEGS
FLVGVAAALSSKSGKIGFVGGMESELIKKFEVGFRAGVQAVNPKAVVEVKYAGGFDKADVGKATAESMYKS
GVDVIYHSAGATGTGVFTEAKNLKKEDPKRDVWVIGVDKDQYAEGQVEGTDDNVTLTSMVKKVDTVVEDVT
KKASDGKFPGGETLTYGLDQDGVGISPSKQNLSDDVIKAVDKWKKKIIDGLEIPATEKELKTFKAE

AdcA (45.14 %)
MFKKWSGLFVIAACFLLVAACGNSSTKGSADSKGDKLHVVTTFYPMYEFTKQIVKDKGDVDLLIPSSVEPH
DWEPTPKDIANIQDADLFVYNSEYMETWVPSAEKSMGQGHAVFVNASKGIDLMEGSEEEHEEHDHGEHEHS
HAMDPHVWLSPVLAQKEVKNITAQIVKQDPDNKEYYEKNSKEYIAKLQDLDKLYRTTAKKAEKKEFITQHT
AFGYLAKEYGLKQVPIAGLSPDQEPSAASLAKLKTYAKEHNVKVIYFEEIASSKVADTLASEIGAKTEVLN
TLEGLSKEEQDKGLGYIDIMKQNLDALKDSLLVKS

BdbD (74.32 %)
MKKKQQSSAKFAVILTVVVVVLLAAIVIINNKTEQGNDAVSGQPSIKGQPVLGKDDAPVTVVEFGDYKCPS
CKVFNSDIFPKIQKDFIDKGDVKFSFVNVMFHGKGSRLAALASEEVWKEDPDSFWDFHEKLFEKQPDTEQE
WVTPGLLGDLAKSTTKIKPETLKENLDKETFASQVEKDSDLNQKMNIQATPTIYVNDKVIKNFADYDEIKE
TIEKELKGK

Qox2 (53.27 %)
MIFLFRALKPLLVLALLTVVFVLGGCSNASVLDPKGPVAEQQSDLILLSIGFMLFIVGVVFVLFTIILVKY
RDRKGKDNGSYNPEIHGNTFLEVVWTVIPILIVIALSVPTVQTIYSLEKAPEATKDKEPLVVYATSVDWKW
VFSYPEQDIETVNYLNIPVDRPILCKISSADSMASLWIPQLGGQKYAMAGMLMDQYLQADKVGTYEGRNAN
FTGEHFADQEFDVNAVTEKDFNSWVKKTQNEAPKLTKEKYDELMLPENVDELTFSSTHLKYVDHGQDAEYA
MEARKRLGYQAVSPHCKTDPFENVKKNEFKKSDDTEE

YxeM (50.38 %)
MKMKKWTVLVVAALLAVLSACGNGNSSSKEDDNVLHVGATGQSYPFAYKENGKLTGFDVEVMEAVAKKIDM
KLDWKLLEFSGLMGELQTGKLDTISNQVAVTDERKETYNFTKPYAYAGTQIVVKKDNTDIKSVDDLKGKTV
AAVLGSNHAKNLESKDPDKKINIKTYETQEGTLKDVAYGRVDAYVNSRTVLIAQIKKTGLPLKLAGDPIVY
EQVAFPFAKDDAHDKLRKKVNKALDELRKDGTLKKLSEKYFNEDITVEQKH

RbsB (29.51 %)
MKKAVSVILTLSLFLLTACSLEPPQWAKPSNSGNKKEFTIGLSVSTLNNPFFVSLKKGIEKEAKKRGMKVI
IVDAQNDSSKQTSDVEDLIQQGVDALLINPTDSSAISTAVESANAVGVPVVTIDRSAEQGKVETLVASDNV
KGGEMAAAFIADKLGKGAKVAELEGVPGASATRERGSGFHNIADQKLQVVTKQSADFDRTKGLTVMENLLQ
GHPDIQAVFAHNDEMALGALEAINSSGKDILVIGFDGNKDALASIKDRKLSATVAQQPELIGKLATEAADD
ILHGKKVQKTISAPLKLETQK

YkwC (89.24 %)
MKKTIGFIGLGVMGKSMASHILNDGHPVLVYTRTKEKAESILQKGAIWKDTVKDLSKEADVIITMVGYPSD
VEEVYFGSNGIIENAKEGAYLIDMTTSKPSLAKKIAEAAKEKALFALDAPVSGGDIGAQNGTLAIMVGGEK
EAFEACMPIFSLMGENIQYQGPAGSGQHTKMCNQIAIAAGMIGVAEAMAYAQKSGLEPENVLKSITTGAAG
SWSLSNLAPRMLQGNFEPGFYVKHFIKDMGIALEEAELMGEEMPGLSLAKSLYDKLAAQGEENSGTQSIYK
LWVK

YeeF (21.04 %)
MKVFEAKTLLSEATDRAKEYKELRTQMVNLRKALKGVADLSDSEFSGKGASNIKAFYTTNVGVADRWIDYI
DMKIAFFNSIAGAAEDKGLSDAYIEESFLEHELANANKKSKSIMSEQKKAMKDILNDIDDILPLDLFSTET
FKDELADANDKRKKTLEKLDALDEDLKTEYALSEPNEQFIKSDFQKLQEATGKGKNATPIHYNAKAYRESD
IHKKRRHLKRRTEAYLKIKKEEAKEREIEKLKERLKNYDYADADEFYEMAKTIGYENLTAEQQRYFTQIEN
TRELEAGFKGVAVGLYDSGKDAVVGLWDMVTDPGGTVEAITGAMAHPIKTYEAISAAIEESYQKDMVNGDT
YSRARWVSYAVGTVVTSIVGTKGVGAVSKTGTAAKVTTKVKTAASKSATAQKAITVSKQTVDHIKQKVNTG
IEVSKKHVKTKLNQIGDLTLADILPYHPRHDLVPAGVPYNAVNGVTLKEGLQKFAKVILPKPYGTSSSGRR
TPAPHVPPVTVKYGEHFARWSRKKVLKPNIIYKTKEGYTYTTDNYGRITSVKADLQLGEAKRNQYAQTNAG
KPQDRKPDDDGGHLIATQFKGSGQFDNIVPMNSQINRSGGKWYEMEQEWAKALSKKPPKKVAVQIEPVYSG
DSLRPSYFDVTYKIGSRKEISVSIKISLGVRRMETRKMQDLYQLIGEKLNDIIPGEWTKIYLYAEVLDDST
MVLFHFRTPENNQIIYSQDIPSHYNVSKDIFKTLLRELRELFEELRTEHRNNNDDVWTNLTLTLDRSGEFQ
LDYNYDDILASELDGYERIAIWEYKNLGILPEDEDDKEFVISYLGL

YpuA (36.21 %)
MKKIWIGMLAAAVLLLMVPKVSLADAAVGDVIVTLGADLSESDKQKVLDEMNVPDNATTVTVTNKEEHEYL
GKYISNAQIGSRAISSSSITIAKKGSGLNVETHNISGITDEMYLNALMTAGVKDAKVYVTAPFEVSGTAAL
TGLIKAYEVSSDEAISEDVKQVANQELVTTSELGDKIGNENAAALIAKIKEEFAKNGVPDNKADIEKQVDD
AASDLNVTLTDSQKNQLVSLFNKMKNADIDWGQVSDQLDKAKDKITKFIESDEGKNFIQKVIDFFVSIWNA
IVSIFK

Table S2: Strain list.

Strain	Genotype	Reference
Bacillus subtilis		
DL1	Wild type (NCIB3610)	(Branda *et al.*, 2001)
DL2	Wild type 168	(Moszer *et al.*, 2002)
DL7	Δ*eps::tet* Δ*tasA::km*	(Lopez *et al.*, 2009c)
DL1308	Δ*ftsH::km*	This study
DL1315	Δ*ftsH::tet*	(Zellmeier *et al.*, 2003)
DL1211	Δ*floT::km*	(Lopez & Kolter, 2010)
DL1442	Δ*floT::spc*	This study
DL1401	Δ*yqfA::mls*	(Lopez & Kolter, 2010)
JS119	Δ*floT* (markerless)	This study
JS152	Δ*yqfA* (markerless)	This study
AY93	Δ*floT::spc*, Δ*yqfA::mls*	This study
DL1419	Δ*floT::km* Δ*yqfA::mls*	This study
JS163	Δ*floT* Δ*yqfA* (markerless)	This study
BM59	*amyE::* P$_{\mathrm{hp}}$-*floT* (*spc*) *lacA*::P$_{\mathrm{hp}}$-*yqfA* (*mls*)	This study
BM28	*amyE::* P$_{\mathrm{hp}}$-*floT* (*spc*)	This study
BM26	*lacA*::P$_{\mathrm{hp}}$-*yqfA* (*mls*)	This study
DL147	Δ*kinC::km*	(Lopez *et al.*, 2009a)
DL227	Δ*kinC::mls*	(Lopez et al., 2009a)
DL1295	*amyE*:: FloT-YFP (*spc*)	(Lopez & Kolter, 2010)
DL1367	*amyE*::YqfA-GFP (*spc*)	This study
AY224	*lacA*::P$_{hp}$-FtsH-RFP (*mls*)	This study
AY225	*lacA*::P$_{ftsH}$-FtsH-RFP (*mls*)	
DL1565	Δ*floT* Δ*yqfA* (markerless) *lacA*::FtsH-RFP (*mls*)	This study
AY238	*amyE*::YqfA-GFP (*spc*) *lacA*:: FtsH-RFP (*mls*)	This study
AY240	*amyE*::FloT-YFP (*spc*) *lacA*:: FtsH-RFP (*mls*)	(Lopez & Kolter, 2010)
DL1056	*lacA*::P$_{hag}$-*cfp* (*mls*)	(Vlamakis et al., 2008)
DL382	*amyE*::P$_{tapA}$-*yfp* (*spc*)	(Vlamakis et al., 2008)
DL1089	*amyE*::P$_{sspB}$-*yfp* (*spc*)	(Vlamakis et al., 2008)
DL1079	*amyE*::P$_{tapA}$-*yfp* (*spc*) *lacA*::P$_{hag}$-*cfp* (*mls*)	(Vlamakis *et al.*, 2008)
DL1521	Δ*ftsH::km amyE*::P$_{tapA}$-*yfp* (*spc*) *lacA*::P$_{hag}$-*cfp* (*mls*)	This study
DL1523	Δ*ftsH::km amyE::*P$_{\mathrm{hp}}$*ftsH(spc) thrC*::P$_{tapA}$-*yfp (cm)* *lacA*::P$_{hag}$-*cfp (mls)*	This study
DL1433	Δ*ftsH::km amyE::*P$_{ftsH}$-*ftsH* (*spc*)	This study
DL1361	Δ*ftsH::km amyE::*P$_{\mathrm{hp}}$-*ftsH* (*spc*)	This study
DL1568	Δ*ftsH::km amyE::*P$_{\mathrm{hp}}$-FtsH-RFP (*spc*)	This study
DL1349	Δ*ftsH::km amyE::*P$_{\mathrm{hp}}$-*ftsH* (*spc*)	This study
DL1404	Δ*ftsH::km amyE::*P$_{\mathrm{hp}}$-FtsH-RFP (*spc*)	This study
DL1461	Δ*ftsH::km amyE::*P$_{\mathrm{hp}}$-*ftsH* (*spc*) *lacA*::P$_{tapA}$-*yfp* (*mls*)	This study
DL1364	Δ*ftsH::km amyE::*P$_{\mathrm{hp}}$-*ftsH* (*spc*) *lacA*::P$_{sspB}$-*yfp* (*mls*)	This study
DL383	Δ*abrB::km*	(Chu et al., 2008)
DL5	Δ*sinR::spc*	(Branda *et al.*, 2006)
DL1148	*amyE::sad67* (*cm*)	(Ireton *et al.*, 1993)
DL1362	Δ*ftsH::tet* Δ*abrB::km*	This study
DL1360	Δ*ftsH::km* Δ*sinR::spc*	This study
DL1363	Δ*ftsH::km amyE::sad67* (*cm*)	This study
DL1372	Δ*floT::spc* Δ*yqfA::mls* Δ*abrB::km*	This study
DL1374	Δ*floT::km* Δ*yqfA::mls* Δ*sinR::spc*	This study

DL1375	Δ*floT::spc* Δ*yqfA::mls amyE*::*sad67* (*cm*)	This study
DL1365	Δ*floT::km* Δ*yqfA::mls,* amyE::*sad67* (*cm*)	This study
DL1430	Δ*rapA::cm* Δ*rapB::spc* Δ*rapE::mls* Δ*spo0E::km*	This study
DL1554	Δ*floT* Δ*yqfA* (markerless) Δ*rapA::cm* Δ*rapB::spc,* Δ*rapE::mls* Δ*spo0E::km*	This study
JS201	Δ*yuaG* (markerless) *amyE*::P$_{hp}$-FloT-His^{6} (*spc*)	This study
JS202	Δ*yqfA* (markerless) *amyE*::P$_{hp}$-YqfA-His^{6} (*spc*)	This study
Other species used in this work		
DL1128	*Staphylococcus aureus* wild type SC-01	(Beenken *et al.*, 2003)
DL95	*Escherichia coli* DH5α	(Reusch *et al.*, 1986)
DL127	*Escherichia coli* DH5α pBR322 P$_{c}$-*gfp*	This study
JC163	*Escherichia coli* DH5α pBR322 P$_{c}$-*rfp*	This study
DL1205	*Pseudomonas aeruginosa* PA14	(O'Toole & Kolter, 1998)

Abbreviations

Antibiotics

mls	Encodes erythromycin + lincomycin resistance protein
km	Encodes kanamycin resistance protein
cm	Encodes chloramphenicol resistance protein
tet	Encodes tetracycline resistance protein
spc	Encodes spectinomycin resistance protein

Protein tags

GFP	Green fluorescent protein
YFP	Yellow fluorescent protein
RFP	Red fluorescent protein
His^{6}	Six histidines

Promoters

P$_{hp}$	Hyperspank IPTG-inducible promoter
P$_{c}$	Constitutive promoter
P*ftsH*	Natural promoter that controls the expression of *ftsH*
P*tasA*	Natural promoter that controls the expression of *tasA*
P*sspB*	Natural promoter that controls the expression of *sspB*
P*hag*	Natural promoter that controls the expression of *hag*

Table S3: Primer list.

Name	Sequence (5’-3’)	Purpose
AY84B	ATGGTGAGCAAGGGCGAGGAGG	Forward RFP
AY85B	TTTTTTGCTAGCTTACTTGTACAGCTCG	Reverse RFP
AY82	TTTTTTGTCGACATGGTACTATTGAACATAGTTGTG	Forward FtsH
AY83B	ATCCTCCTCGCCCTTGCTCACCATCTCTTTCGTATCGTCTTTC	RFP tail
AY132	TGCTAAGCTTACATAAGGAGGAACTACTATGACAATGCCGATTAT	Forward FloT
AY133	ATCCTCCTCGCCCTTGCTCACCATCTCTGATTTTTGGATCGTTT	Reverse FloT (LFH) RFP
AY134	TTTTTGGATCCTTACTTGTACAGCTCGTCCAT	Reverse RFP (BamH1)
Ftshfwsal	AAAAGTCGACATGGTACTATTGAACATAGTTGT	Forward IPTG-controlled FtsH
Ftshrvsph	AAAAGCATGCTGATTGTAAAAGCCGCAGC	Reverse IPTG-controlled FtsH
Pftshfw	TTTTGAATTCAACGAGCGAGTATCAAGATACA	Forward Promoter *ftsH*
Pftshrv	TTTTAAGCTTTCCTTACCTCCTCCCACAGT	Reverse Promoter *ftsH*
Ftsh1	CAGCGACCGCATTGTATT	Δ*ftsH* cassette
Ftshkm2	CCTATCACCTCAAATGGTTCGCTGCCGATCAGCTTTCATAA	Δ*ftsH* cassette
Ftshtet2	GAGAACAACCTGCACCATTGCAAGATGCCGATCAGCTTTCATAA	Δ*ftsH* cassette
Ftshkm3	CGAGCGCCTACGAGGAATTTGTATGCTGCCAAGAGAAGACCGTT	Δ*ftsH* cassette
Ftshtet3	GGGATCAACTTTGGGAGAGAGTTCTATGCTGCCAAGAGAAGACCGTT	Δ*ftsH* cassette
Ftsh4	AGCTTTGCTGCACGCGA	Δ*ftsH* cassette
AY86	ATTTGCAGCATATCATGGCGTG	Δ*pbpE* cassette
AY87	CTTGATAATAAGGGTAACTATTGCCCCTCCACCTCCCATATCTCTG	Δ*pbpE* cassette
AY88	GGGTAACTAGCCCTCGCCGGTCCACGAAAGGAATGAATGAATTTGATGATCGG	Δ*pbpE* cassette
AY89	AGCTTTGATAAGCAAGATATGTG	Δ*pbpE* cassette
JS15	TTTTGGATCCCCATTTSTAAAGCACTTCAAATGG	Flotfw1
JS16	AGTTACCATACGGTTCTGCCCCAAATTCCTCCTCCTTTTTATGTAAAATG	Flotrv2
JS17	GGGCAGAACCGTATGGTAACTG	Flotfw3
JS18	TTTTGTCGACCTTTAACTTATAATGCGACTTAC	Flotrv4
JS19	TTTTGGATCCCCAGATCAGCTATGCAAAGGAG	Yqfafw1
JS21	GCGTTCTCCCTTCTTAGAGAGGTTGACGGACCCATATAACTTC	Yqfarv2
JS22	CTCTCTAAGAAGGGAGAACGC	Yqfafw3
JS39	TTTTGTCGACCAGATATGATGCAGTGGCCCTG	Yqfarv4
BM5	AAAAGTCGACTAAGGAGGAACTACTATGACAATGCCGATTATAAT	Forward IPTG-controlled FloT
BM6	AAAAGCATGCTTACTCTGATTTTTGGATCG	Reverse IPTG-controlled FloT
BM7	AAAAGTCGACTAAGGAGGAACTACTATGGATCCGTCAACACTTA	Forward IPTG-controlled YqfA
BM8	AAAAGCATGCTTATGATTTGCGGTCTTCAT	Reverse IPTG-controlled YqfA
JS44	AAAAGCATGCTTAGTGATGATGATGATGATGGCTGCTCTCTGATTTTTGGATCG	FloT Reverse (His6)
JS45	AAAAGCATGCTTAGTGATGATGATGATGATGGCTGCTTGATTTGCGGTCTTCAT	YqfA Reverse (His6)

Reference list

Beenken, K. E., J. S. Blevins & M. S. Smeltzer, (2003) Mutation of sarA in Staphylococcus aureus limits biofilm formation. *Infect Immun* **71**: 4206-4211.

Branda, S. S., F. Chu, D. B. Kearns, R. Losick & R. Kolter, (2006) A major protein component of the Bacillus subtilis biofilm matrix. *Mol Microbiol* **59**: 1229-1238.

Branda, S. S., J. E. Gonzalez-Pastor, S. Ben-Yehuda, R. Losick & R. Kolter, (2001) Fruiting body formation by Bacillus subtilis. *Proc Natl Acad Sci U S A* **98**: 11621-11626.

Chu, F., D. B. Kearns, A. McLoon, Y. Chai, R. Kolter & R. Losick, (2008) A novel regulatory protein governing biofilm formation in Bacillus subtilis. *Mol Microbiol* **68**: 1117-1127.

Ireton, K., D. Z. Rudner, K. J. Siranosian & A. D. Grossman, (1993) Integration of multiple developmental signals in Bacillus subtilis through the Spo0A transcription factor. *Genes Dev* **7**: 283-294.

Lopez, D., M. A. Fischbach, F. Chu, R. Losick & R. Kolter, (2009a) Structurally diverse natural products that cause potassium leakage trigger multicellularity in Bacillus subtilis. *Proc Natl Acad Sci U S A* **106**: 280-285.

Lopez, D. & R. Kolter, (2010) Functional microdomains in bacterial membranes. *Genes Dev* **24**: 1893-1902.

Lopez, D., H. Vlamakis, R. Losick & R. Kolter, (2009b) Cannibalism enhances biofilm development in Bacillus subtilis. *Mol Microbiol* **74**: 609-618.

Lopez, D., H. Vlamakis, R. Losick & R. Kolter, (2009c) Paracrine signaling in a bacterium. *Genes Dev* **23**: 1631-1638.

Moszer, I., L. M. Jones, S. Moreira, C. Fabry & A. Danchin, (2002) SubtiList: the reference database for the Bacillus subtilis genome. *Nucleic Acids Res* **30**: 62-65.

O'Toole, G. A. & R. Kolter, (1998) Flagellar and twitching motility are necessary for Pseudomonas aeruginosa biofilm development. *Mol Microbiol* **30**: 295-304.

Reusch, R. N., T. W. Hiske & H. L. Sadoff, (1986) Poly-beta-hydroxybutyrate membrane structure and its relationship to genetic transformability in Escherichia coli. *J Bacteriol* **168**: 553-562.

Vlamakis, H., C. Aguilar, R. Losick & R. Kolter, (2008) Control of cell fate by the formation of an architecturally complex bacterial community. *Genes Dev* **22**: 945-953.

Zellmeier, S., U. Zuber, W. Schumann & T. Wiegert, (2003) The absence of FtsH metalloprotease activity causes overexpression of the sigmaW-controlled pbpE gene, resulting in filamentous growth of Bacillus subtilis. *J Bacteriol* **185**: 973-982.